DOI: 10.7409/rabdim.026.001

GRZEGORZ MAZUREK [1)]
ORCID: 0000-0002-9735-1725

PRZEMYSŁAW BUCZYŃSKI [2)]
ORCID: 0000-0003-0798-8093

MAREK IWAŃSKI [3)]
ORCID: 0000-0002-0414-682X

ARTUR KOWALCZYK [4)]
ORCID: 0009-0005-1889-3382

MARCIN PODSIADŁO [5)]
ORCID: 0000-0002-9188-3472

MATÚŠ KOZEL [6)]
ORCID: 0000-0003-4176-1394

Impact of recycled glass and carbon geogrids on crack propagation resistance in asphalt concrete

Abstract: The paper analyses the impact of recycled geogrid fibres on the mechanical and physical properties of asphalt concrete. Survey results indicate that the knowledge in this area is very limited. The presence of geogrid fibres from milling is an increasingly common challenge for the design of new pavements from asphalt mixtures containing recycled asphalt pavement. The adopted research procedure provided for the selection and optimisation of the content of recycled glass and carbon geogrids added to the asphalt mixture. Two reference asphalt concrete mixtures for the binder course were designed: AC 16W 35/50 KR3-4 and AC 22W 35/50 KR3-4. The research process was controlled using a factorial experiment design, including two qualitative variables: geogrid type and grain size distribution in the asphalt mixture, and two qualitative variables: share and length of geogrid fibres. The mixtures designed and prepared under laboratory conditions were subject to the test of crack propagation resistance using the SCB method. The research also included an assessment of associated properties: air void content V_a, water resistance *ITSR* and rutting resistance PRD_{air}, WTS_{air}. The results of the analysis indicated a potential way to improve the fracture toughness of asphalt concrete for the binder courser by optimising geogrid parameters. Also, the potential use of recycled geogrid to make asphalt mixtures enables the implementation of sustainable development principles in the road construction sector.

Keywords: experiment design, fracture toughness, optimisation, recycled geogrid, recycling.

[1)] Kielce University of Technology, Faculty of Civil Engineering and Architecture, 7 Tysiąclecia Państwa Polskiego Av., 25-314 Kielce, Poland; gmazurek@tu.kielce.pl (✉)
[2)] Kielce University of Technology, Faculty of Civil Engineering and Architecture, 7 Tysiąclecia Państwa Polskiego Av., 25-314 Kielce, Poland; p.buczynski@tu.kielce.pl
[3)] Kielce University of Technology, Faculty of Civil Engineering and Architecture, 7 Tysiąclecia Państwa Polskiego Av., 25-314 Kielce, Poland; iwanski@tu.kielce.pl
[4)] Kielce University of Technology, Faculty of Civil Engineering and Architecture, 7 Tysiąclecia Państwa Polskiego Av., 25-314 Kielce, Poland; akowalczyk@tu.kielce.pl
[5)] Kielce University of Technology, Faculty of Civil Engineering and Architecture, 7 Tysiąclecia Państwa Polskiego Av., 25-314 Kielce, Poland; mpodsiadlo@tu.kielce.pl
[6)] University of Žilina, Faculty of Civil Engineering, 8215/1 Univerzitná St., 010 26 Žilina, Slovakia; matus.kozel@uniza.sk

Article is distributed under the terms of the Creative Commons Attribution 4.0 International License **(CC-BY 4.0)**

1. INTRODUCTION

The aim of circular economy is to create a closed loop in which waste is regarded as recyclable materials. Products and materials circulate in the economy as long as possible, significantly contributing to sustainable development and reducing the negative environmental impact of the construction industry [1]. Examples of waste materials commonly used in the road construction industry include recycled asphalt pavement, which is produced by milling renovated asphalt pavements [2]. The WT-2/2014 document [3] specifies the requirements for processed RAP (reclaimed asphalt pavement), which are referred to as recycled asphalt pavement once their quality is proved and they become an ingredient for the production of hot-mix asphalt (HMA). Significant aspects of the quality assessment of recycled asphalt pavement include the content of foreign matter, particularly of the second group, which includes (among others): plastics, synthetic materials and wood [4]. Fragments of geogrid fibres, which increasingly appear in recycled asphalt pavement after the milling of flexible pavement [5], are considered by the currently applicable technical codes to be foreign matter – impurities [3, 4]. Geogrids used to strengthen the layers of asphalt pavements are made of glass and carbon fibres, which should be qualified as a non-natural, chemical and inorganic material [6]. According to the authors of the paper [7], using recycled fibres could significantly reduce the costs connected with the use of this material for asphalt mixture production and help to revise the approach to this modification of asphalt concrete (AC). In tests [8] performed locally in Germany for S&P Clever Reinforcement GmbH, it was proven that the glass and carbon geogrid exhibits very good behaviour during pavement milling after the end of its service life. It was established that the milled product could be fully suitable for reuse in the asphalt mixture according to the statutory German codes [9]. The rutting resistance tests, in turn, showed that fragments of a specific S&P Glass/Carbonphalt G geogrid did not have a negative effect on the properties of asphalt concrete.

The content of synthetic materials in the recycled asphalt pavement to be used for the production of the asphalt mixture dedicated to the binder course in the road pavement structure had to be lower than a specific limit, i.e., 0.1% of the weight of recycled asphalt pavement added to the asphalt mixture [3]. The problem of RAP being contaminated with geosynthetic fibres is growing because glass and carbon geogrid is increasingly used in maintenance activities. This increases the amount of waste geogrid and RAP – as the carrier of impurities in the form of geogrid fragments. RAP that do not meet the requirements of the relevant standards in this regard give rise to the technical question regarding the feasibility of their reuse. The issue of the impact of reinforcing fibres on the service life of asphalt mixtures is often discussed in research papers, but this discussion mostly concerns new fibres [7]. New fibres are not regarded as impurities by the supervisory authorities, which is a different approach to the one regarding the fibres from the recycled geogrid [4]. New fibre reinforcement is regarded as a legitimate additive that improves physical, mechanical and fatigue properties of asphalt mixtures [7]. Fibre reinforcement in the asphalt mixture is considered to be incidental by some [10], but most researchers believe that the fibres function as a bridge in cracks, absorbing, redistributing and transferring stresses to prevent or delay crack propagation [11-13]. To the best of the knowledge of the authors, despite numerous and advanced studies of the impact of fibre reinforcement on asphalt mixture properties in research papers worldwide, there are no adequate studies of the impact of recycled glass and carbon geogrid fibres.

The research objective of the study was to assess if foreign matter in RAP in the form of geogrid fibres > 0.1%, with a size of 1 cm, 3 cm and 5 cm, added to asphalt concrete could enable the effective use of the potential of the recycled geogrid. The analyses were carried out with a particular focus on the impact of recycled fibres on mechanical and physical properties, including the fracture toughness of asphalt pavements intended for the binder course for the KR3-4 traffic volume category.

2. SURVEY

Since the recycling of the geogrid after the end of its service life has not been investigated in Poland, the assessment of the impact of recycled fibres has been extended to include a survey, which was a key stage of the

research work, preceding laboratory tests. The awareness of sustainable development increases in parallel with the demand for sustainable products and technologies, which has been confirmed in the research survey conducted in 2023 [5]. A survey with 16 questions was used to analyse the expectations and observations concerning the presence of impurities in RAP. The respondents included parties from all over Poland, such as: road operators, research centres (universities and secondary schools), design contractors, client's engineers and, most importantly, persons directly involved in the production of asphalt mixtures and the construction of asphalt pavements. The distribution of the number of respondents by province is shown in Fig. 1 [5, 14].

The primary objective of the survey was to determine the needs and problems faced by the parties involved in the construction process that handle RAP with geogrids. Specific information can be found in the paper [14]. However, the reasons to conduct the research were defined by the following questions: What impurities are most often found in RAP? According to the respondents, the most common type of impurities in RAP were materials from the aggregate sub-base. This answer was given by 61.4% of the survey-takers. Another important aspect was the identification of the second-largest group of impurities, i.e., geogrids. This type of impurities was indicated by 53.2% of the survey-takers. The share of answers to the above-mentioned question is given in Fig. 2.

Fig. 1. Number of respondents by voivodeship

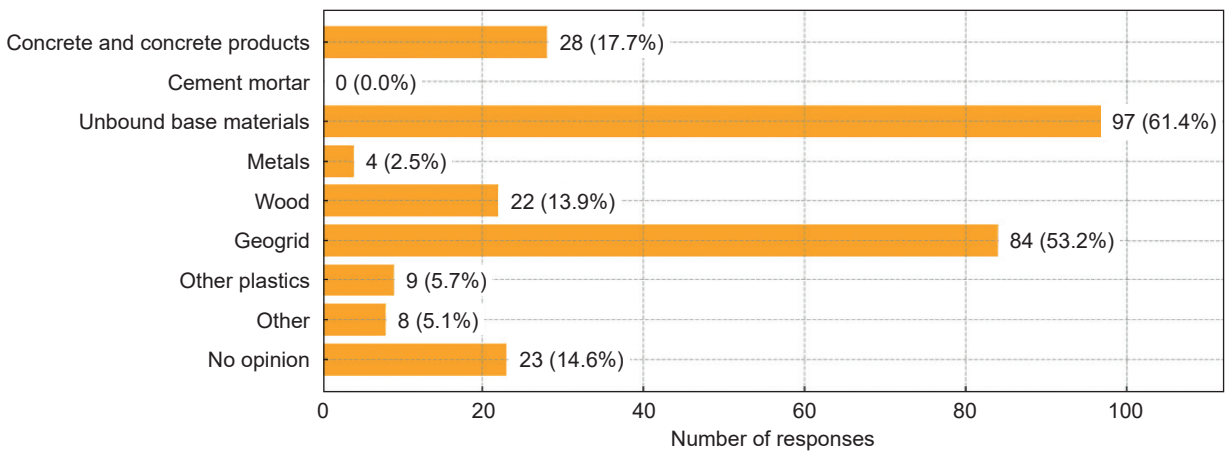

Fig. 2. Share of respondent answers

3. MATERIALS AND METHODS

3.1. GEOGRID

In connection with the research, micro- and macro-fibres of G 100/100 glass geogrid and Carbon-Carbon 100/100 carbon geogrid were introduced into the asphalt mixture. The geogrids used to obtain the fibres are intended for use in asphalt pavements and overlays, fulfilling the requirements of PN-EN 15381 [15]. In the research, the geogrid fibres were selected based on factors such as fibre length and their simulated ageing, and they were processed in a Los Angeles drum, similarly to what the researchers did in the paper [8]. The procedure for obtaining the appropriate lengths of the geogrid fibers was conducted manually by cutting the geogrid into segments of 1 cm, 3 cm, and 5 cm and subsequently verifying their lengths. Within the LA drum, solely the aging process of fibers that had been adequately prepared, namely trimmed, was executed. The purpose of the aging process in the LA drum was to simulate the long-term functionality of the geogrid within the asphalt surface and the surface milling procedure performed during the final phase of the geogrid's utilization, during which fragments of the geogrid are produced, leading to contamination of the reclaimed asphalt. The determination of the number of rotations of the LA drum and the quantity of fiber doses subjected to the aging process was established experimentally through multiple comparisons of various visual observations of real fibers sourced from numerous road surfaces post-milling process and new fibers aged in the laboratory. To achieve the most precise representation of the geogrid's operational lifespan in the pavement, results from local research conducted in Germany were also considered [8].

3.2. ASPHALT CONCRETE DESIGN

The design of the asphalt mixtures was preceded by a detailed analysis of all the mineral ingredients, RAP, bituminous binder and added glass and carbon geogrid fibres for conformity to the requirements of the standards for asphalt mixture materials. The composition of the asphalt mixture was designed using the limit curve method. The grain size limit curves used in the tests of the asphalt mixtures: AC 16W KR3-4 and AC 22W KR3-4 are shown in Fig. 3a and 3b.

Based on the limit curves determined in technical guidelines WT-2/2014, it was assumed that the reference asphalt mixture AC 16W would contain 20% RAP (11.2 GRA 0/8.0), 37% 8/16 mm coarse aggregate, 21% 2/8 mm coarse aggregate, 21% 0/2 fine aggregate and 1.0% limestone filler. The designed reference asphalt concrete mixture AC 22W contained 20% RAP (22.4 GRA 0/16), 22% 16/22 mm coarse aggregate, 20% 8/16 mm coarse aggregate, 16% 2/8 mm coarse aggregate, 21% 0/2 fine aggregate and 1.0% limestone filler. Asphalt mixtures were made using 35/50 paving-grade bitumen in the amount of 3.7% (AC 16W) or 3.4% (AC 22WP). The remaining required amount of total asphalt was made up by the asphalt contained in the RAP, which amounted to 0.9% for the AC 16W mixture and 1.0% for AC 22W.

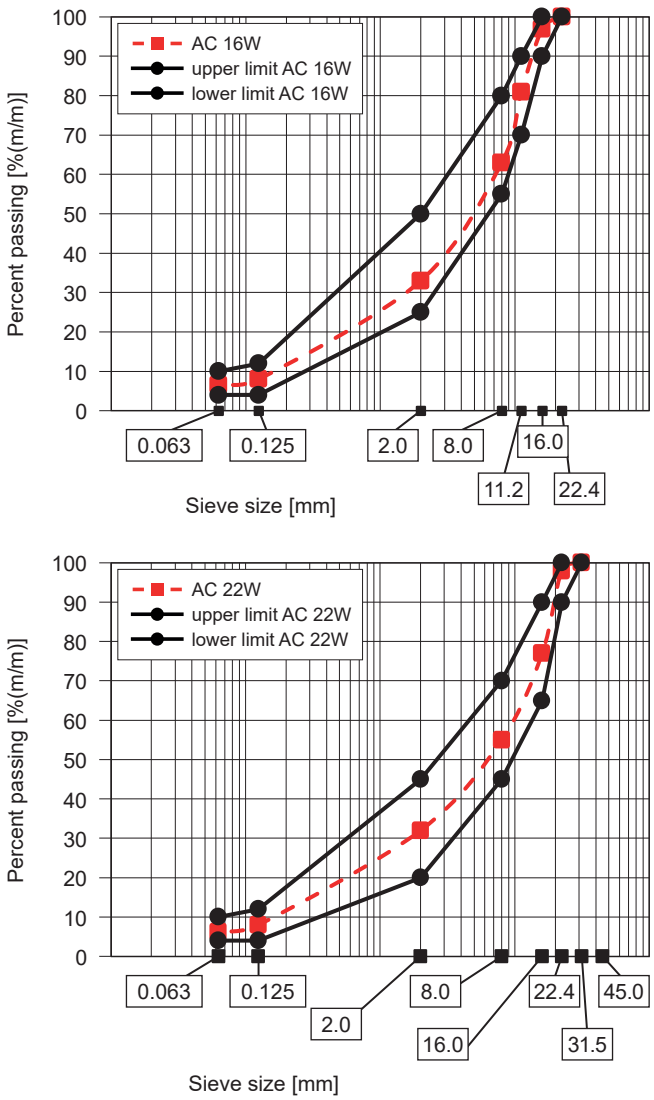

Fig. 3: Grain size limit curves for the asphalt concrete (AC) mixtures: a) AC 16W KR3-4, b) AC 22W KR3-4

3.3. EXPERIMENT PLAN

A critical part of every experiment was the selection of the correct sampling system. The impact of geogrid fibres on asphalt concrete properties was assessed using the classical factorial experiment design[16, 17]. The starting topology for the experiment design was a plan with different input values. The range of controlled qualitative input variables for the share of geogrid fibres was determined based on the analysis of research papers assessing the impact of fibre reinforcement, particularly glass and carbon fibres, on the properties of hot mix asphalt (HMA) [8]. The qualitative variables concerning the fibre length were considered with reference to the results of respondent answers from the research survey, the analysis of scientific papers and own experience from past observations. The analysis usually covered the shape, diameter and length of the fibres in the RAP. The input variables for the experiment consisting of independent, controlled variables are given in Table 1.

Table 1. Input variables and their levels in the experiment design

Quantitative variable	Levels	Qualitative variables	Levels
Geogrid share [%]	0.2, 0.6, 1.0	Geogrid type	Carbon, glass
Geogrid length [cm]	1, 3, 5	Asphalt mixture type	AC 16W, AC 22W

Two quantitative variables were introduced on 3 levels, and the remaining two qualitative variables were introduced on 2 levels. Additional coding was required for the qualitative variables. This was necessary in order to build a regression model determined based on a generalised linear model (GLM) algorithm, extensively described in the paper [18]. Consequently, the AC 16W mixture was assigned the value 0, and AC 22W was coded as 1. The same method was used to code the levels of the geogrid type variable: carbon geogrid 1 and glass geogrid 0. For the quantitative variables, the authors also considered non-linear effects because the number of levels permitted this > 2. The number of combinations was due to the adopted form of the regression model and adopted limitations. The primary limitation was the absence of the non-linear impact of qualitative variables. Most importantly, the adopted model enabled the assessment of interactions between the qualitative and quantitative variables.

The final regression model had the following general formula (1):

$$y = b_0 + b_1 x_1 + \cdots b_k x_k + b_{12} x_1 x_2 + \\ + \cdots + b_{k-1.k} x_{k-1} x_k + \cdots + b_{11} x_1^2 + b_{kk} x_k^2, \quad (1)$$

where:

b_k – experimental factors,
x_k – variables,
y – dependent variable.

With consideration of the limitations mentioned above, the modified model (1) was subject to further evaluation. The basic factorial plan was optimised using the criterion of *G*-optimality, defined as a plan that minimises the largest standard deviation of the determinable response surface (dependent variable determined from the approximating function). As a result, to meet the conditions for value maximisation according to the *G*-optimality criterion, an experiment design was developed with 14 combinations. The number of replications resulted from the standard requirements according to which this study was implemented. The experiment domain used in the study is shown in Table 2.

Table 2. Experiment domain

Item	Geogrid type	Asphalt mixture type	Percentage of fibers by mass [%]	Fibre length [cm]
1	glass	AC 16W	0.2	1
2	glass	AC 16W	0.6	3
3	glass	AC 16W	1.0	5
4	glass	AC 22W	0.2	1
5	glass	AC 22W	1.0	5
6	carbon	AC 16W	0.2	1
7	carbon	AC 16W	0.6	3
8	carbon	AC 16W	1.0	5
9	carbon	AC 22W	0.2	1
10	carbon	AC 22W	0.6	3
11	carbon	AC 22W	1.0	5
12	carbon	AC 22W	1.0	1
13	carbon	AC 16W	0.2	5
14	glass	AC 22W	0.2	5

3.4. PHYSICAL AND MECHANICAL PROPERTIES OF ASPHALT CONCRETE

The study of the impact of asphalt concrete modification with selected geogrid fibres began with basic standard tests. The following is a list of the basic tests with relevant standards and codes (Table 3).

Table 3. Basic tests of asphalt concrete

No.	Tested parameters	Standard
1	Air void content in the asphalt mixture V_a	PN-EN 12697-8 [19]
2	Water resistance *ITSR*	PN-EN 12697-12 [20], annex 1 to WT-2 part I [3]
3	Water absorption *Nw*	PN-EN 1097-6 [21]
4	Indirect tensile strength ITS_{dry}	PN-EN 12697-23 [22]
5	IT-CY stiffness modulus at: −10°C, 5°C, 13°C, 25°C, 50°C	PN-EN 12697-26 [23]
6	Rut growth rate WTS_{air} [mm/1000 cycles], small apparatus, method B, in air, 60°C, 10,000 cycles	PN-EN 12697-22 [24]

3.5. SCB FRACTURE TOUGHNESS

The main part of the tests was the assessment of asphalt concrete in the context of its fracture toughness. The analysis of fracture toughness using the SCB (Semi-Circular Bending) method with a semi-cylindrical specimen with a central notch aims to assess the properties of the material, in this case: asphalt mixtures reinforced with geogrid fibres, regarding the resistance to the loads that lead to the appearance and propagation of cracks. This test can be used to determine the strength parameters of the asphalt mixture, including the resistance to dry and fatigue cracking, which is critical to the durability of road pavements. Crack propagation in the semi-circular bending test was measured using specimens of AC 16W 35/30 KR3-4 and AC 22W 35/50 KR3-4 asphalt concrete, according to test standard PN-EN 12697-44 [25]. The specimens for the tests were obtained from cores cut out of slabs formed at a laboratory with a thickness of 50 mm (± 3 mm). The slabs were formed using a laboratory roller according to the requirements of PN-EN 12697-33 [26]. Every specimen had the shape of a semi-cylinder with a diameter of 150 mm (± 1 mm). In the central part of the flat base of the specimen, a notch was made with the nominal width of 1.00 mm (± 0.10 mm) and a depth of 10 mm (± 1.0 mm), which simulated initial cracking. Before the tests, the specimens were kept in a climate chamber for 4 h under the conditions defined in PN-EN 12697-44 to ensure uniform testing conditions. During the experiment, the specimens were placed in a special test frame (Fig. 9), which enables the application of a three-point bending load. The measurement was conducted at 0°C. The load was applied vertically via the top support, which generated tensile stresses at the bottom of the specimen. The strain growth rate was constant and amounted to 5 mm/min (± 0.2 mm/min). The load increased gradually until it reached the maximum value F_{max} at which specimen failure occurred. The test for every replication was conducted on a set of 6 specimens, which produced valid results for at least 4 specimens. The fracture toughness K_{Ic} of the specimen was calculated according to formulas (2-3):

$$K_{Ic,i} = \sigma_{max,i} \cdot Y \cdot \sqrt{\pi \cdot a_i} \, \frac{N}{\text{mm}}^{\frac{3}{2}}, \tag{2}$$

$$Y = 4.782 - 1.219 \cdot (\frac{a_i}{r_i}) + 0.063 exp\ [7.045 \cdot (\frac{a_i}{r_i})], \tag{3}$$

where:

a_i – the cracking depth of specimen i, i = 1, ..., 4, [mm],

$\sigma_{max,i}$ – the failure load of specimen i, i = 1, ..., 4, [N/mm^2],

Y – the normalised stress intensity factor.

The *J*-integral, also referred to as the Rice integral [27], is one of the key parameters used in fracture mechanics to assess the resistance of materials to crack propagation. In the context of the fracture toughness of the asphalt mixture using the SCB method according to PN-EN 12697-44 [25], the *J*-integral is used to determine the energy required for crack initiation and propagation in the tested specimen. The *J*-integral describes the intensity of the stress field and the strain energy in the material near the crack front. In practice, it can be used to determine the fracture toughness of the asphalt mixture. The higher the value of *J*, the higher the capacity of the material to absorb energy before the crack propagates, suggesting its increased durability and resistance to damage. A lower value of the *J*-integral indicates a more brittle material with a higher susceptibility to cracking. The *J*-integral can be used to predict the durability of the pavement, enabling a quantitative assessment of the capacity of the material to absorb energy and prediction of the service life in the operating conditions because a high value of *J* indicates an improved resistance to fatigue and thermal damage [28, 29]. This method is widely used in road engineering to optimise the content of the asphalt mixture and improve the service life of the pavement. The value of the *J*-integral was calculated according to the formula (4):

$$J = \frac{2 \cdot (0.5 \cdot F_{max,i} \cdot \Delta W_i)}{t_i \cdot (W_i - a_i)} \cdot [\frac{kJ}{m^2}], \tag{4}$$

where:

$F_{max,i}$ – the maximum load of specimen i, i = 1, ..., 4, [N],

Δ_{Wi} – the vertical strain at the maximum load for specimen i, i = 1, ..., 4, [mm],

t_i – the thickness of specimen i, i = 1, ..., 4, [mm],

W_i – the height of specimen i, i = 1, ..., 4, [mm],

a_i – the cracking depth of specimen i, i = 1, ..., 4, [mm].

In the publication [30], the authors analysed the fracture toughness of the asphalt mixture according to PN-EN 12697-44, using the fracture toughness parameter K_{Ic} [31]. They showed that the value of the parameter was associated with the maximum stress the material could withstand before failure, contributing to the use of rigid asphalt mixtures. In the analysis, they pointed out that where asphalt overlays were used on old, cracked pavement layers, excessively rigid mixtures could be a sub-optimal solution because a base with a reduced stability required a material capable of compensating for base movement. The observation of the authors, which undermines the feasibility of using rigid asphalt layers as overlays of renovated roads, highlights the significance of the deformability of the mixture at the maximum failure load. Since asphalt mixtures used in binder courses are also exposed to tensile stresses, deformability is also an important parameter. To effectively assess the interdependence of maximum strain $\varepsilon_{max,i}$ and fracture toughness K_{Ic} for the verification of the properties of asphalt concrete AC 16W and AC 22W modified with geogrid fibres, the authors used indicator P developed by the authors of the paper [30], defined with the following formula (5):

$$P = K_{Ic} \cdot \varepsilon_{max,i}. \quad (4)$$

4. TEST RESULTS AND DISCUSSION

4.1. IMPACT OF RECYCLED GEOGRID ON THE PHYSICAL PROPERTIES OF ASPHALT CONCRETE

The assessment of the impact of recycled geogrid on asphalt concrete is a complex issue. The actual number of the effects of interactions between the predictors is not known, but it may be imposed by the adopted sampling system. The use of the topology depends, as indicated earlier, on interaction effects. However, the organisation of combinations between the predictors in space can also be useful for the application of clustering techniques. This gives a guarantee that representative cases/combinations enable the correct classification of the specimens into homogeneous groups. The clustering technique provides generalised conclusions similar to the ones provided by the regression method. Consequently, the authors first aggregated the central measures and scatter of all the combinations of selected physical properties of asphalt mixtures: V_a and ρ_{ssd}. The initial redundancy assessment was carried out using a module implemented in Statistica. The main criterion for the analysis was to identify the properties correlated with each other with a ratio r = 0.8 for quantitative features and Cramér's V = 0.8 for qualitative properties. The analysis identified a strong correlation of V_a with N_w and ρ_{ssd}. Consequently, Fig. 4 only shows the results of the distribution of the following properties: V_a and ρ_{ssd}.

The results in Fig. 4 indicate that a fibre content up to 0.2% with the smallest length of 1 cm decreased the air void content Va and increased the bulk density ρ_{ssd}. This suggests that a small quantity of fibres improved the compaction of asphalt concrete. However, if the fibre length was consistently increased, this reduced the bulk density of asphalt concrete and increased the air void content. Thus, the increase of recycled geogrid > 0.6% hindered the compaction of the mixtures and resulted in a large scatter of test results. When all the results for asphalt concrete mixtures containing recycled geogrid fibres > 0.6% are compared, it can be found that the median of the property V_a is lower than for the reference mixtures.

4.2. IMPACT OF RECYCLED GEOGRID ON THE MECHANICAL PROPERTIES OF ASPHALT CONCRETE

A very important aspect was also the description of the mixtures with the recycled geogrid in terms of the distribution of asphalt concrete stresses and strains. In this context, the authors determined the stiffness moduli at temperatures from −10°C to 50°C. All the stiffness moduli were subject to an assessment of redundancy, similarly to the procedure followed for the physical properties. The analysis of the correlation of *Sm* showed that the stiffness moduli determined in the indirect tensile test at different temperatures were correlated with each other. The reason for this is that their measurement was conducted in the linear viscoelastic range, where the Boltzmann superposition principle applied. Thus, the value of the stiffness moduli was a combination of the measurement temperature factor. To illustrate the distribution of the *Sm* property, the authors aggregated the values of the *Sm* property vs temperature (Fig. 5).

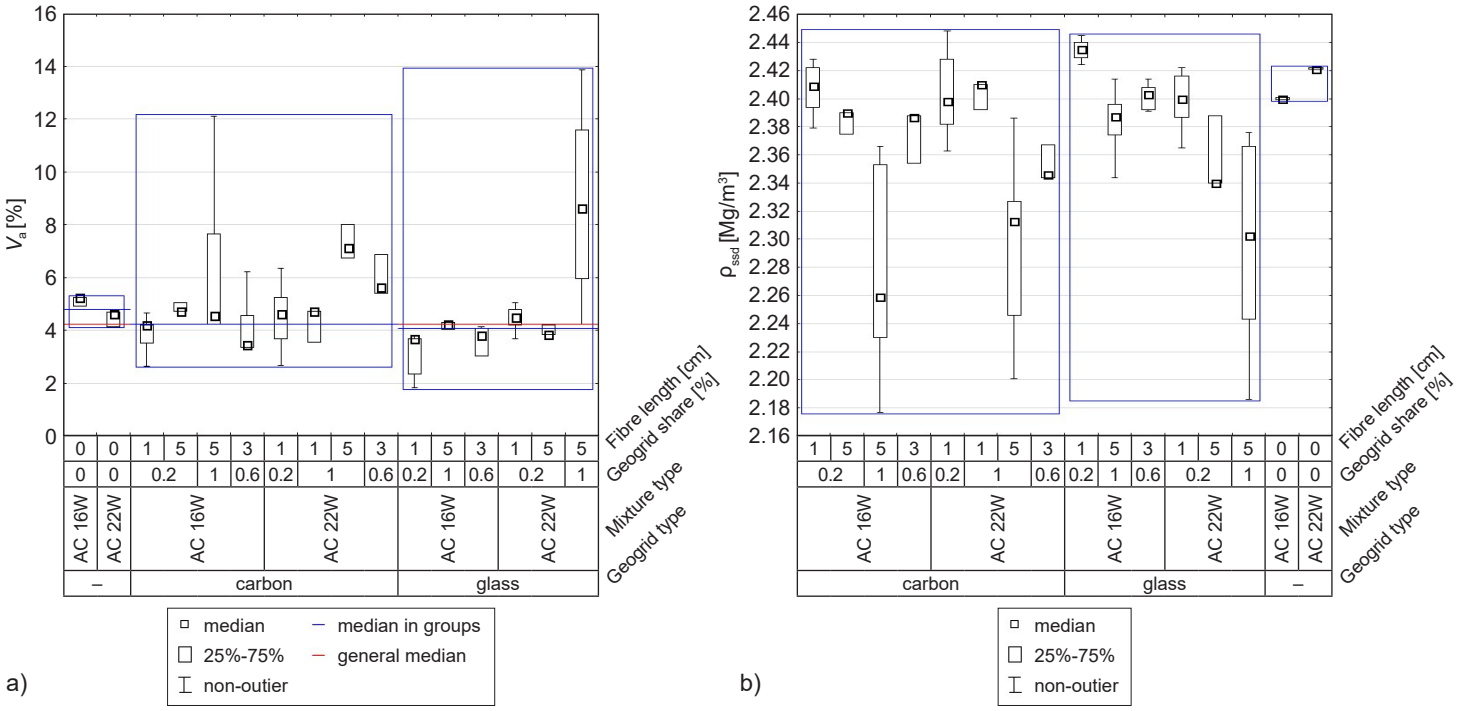

Fig. 4. Physical properties of asphalt concrete for the binder course: a) V_a, b) ρ_{ssd}

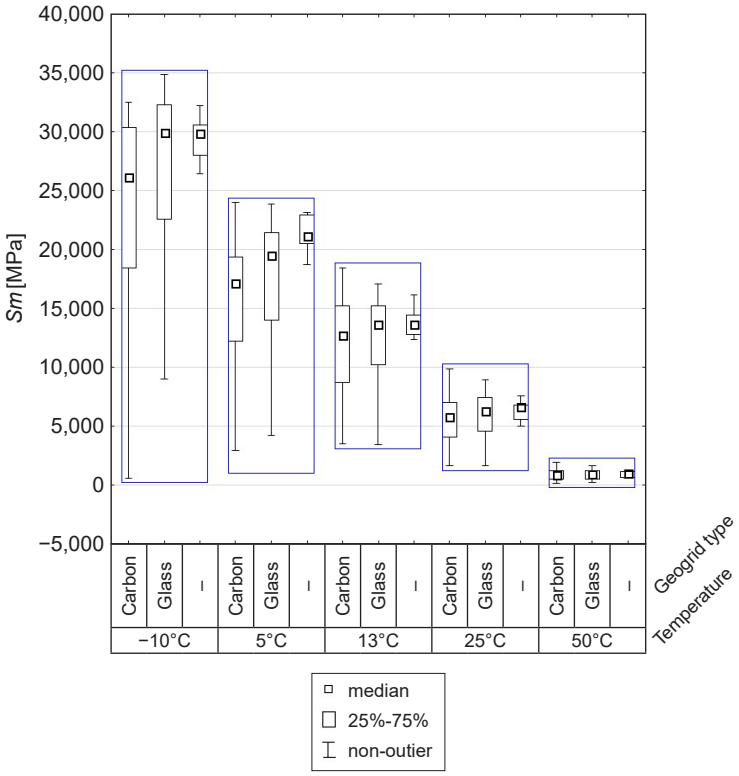

Fig. 5. Stiffness modulus *Sm* vs temperature broken down into geogrid types

The results in Fig. 5 show that, similarly to other thermoplastic materials, the stiffness modulus decreases along with an increase in temperature. The scatter of results increased along with the decrease in measurement temperature, showing a strong synergy of the binder with the parameters of the recycled geogrid. A comparison of the median of *Sm* at 13°C, which amounted to 13,187 MPa, and its value adopted in the Book of Typical Flexible and Composite Pavements (KTKNPiP) [32], i.e., 10,300 MPa, shows that the observed value was slightly elevated. Higher values of the stiffness modulus *Sm* help to reduce the strain in the pavement structure in which this asphalt concrete with the recycled geogrid will be implemented. In the case of the glass geogrid, there was no significant decrease in the average stiffness modulus of the asphalt concrete in comparison with the reference asphalt concrete mixtures. However, it was also very important to determine if the use of the recycled geogrid would not decrease the cohesion of the asphalt concrete ITS_{dry} and result in a high rut growth rate WTS_{air} during simulated rutting. The results of the determination of these two properties are shown in Fig. 6.

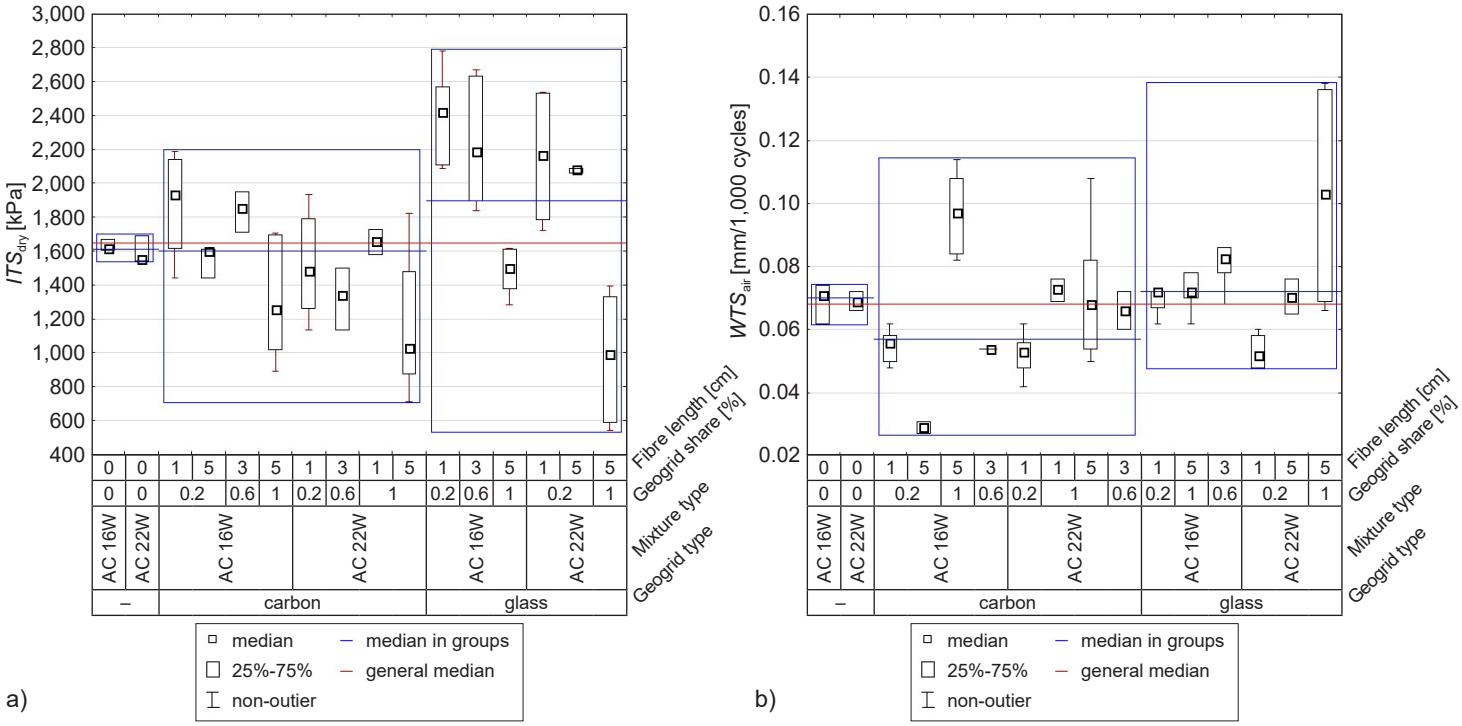

Fig. 6. Distribution of selected mechanical properties: a) ITS_{dry}, b) WTS_{air}

It should be noted that the average level of ITS_{dry} (Fig. 6a) for the carbon geogrid does not deviate from the median of all results in the experiment or from the median for the reference mixtures. For the carbon geogrid, the highest ITS_{dry} was observed for the geogrid share of 0.2% with a fibre length of 1 cm regardless of the grain size distribution of asphalt concrete. For the glass geogrid, the indirect tensile strength was 14% higher than the general median of all the results in the experiment. The increase in this parameter was particularly noticeable in the results for glass geogrid with a share of 0.2%. ITS_{dry} decreased radically when the fibre length was 5 cm. Thus, the relationship between fibre length and grain size distribution should be considered when designing the asphalt mixture [33].

Regarding the creep rate WTS_{air}, the effect of geogrid type was more advantageous in the case of the carbon fibre geogrid (Fig. 6b). The reason for this is that the carbon geogrid has a higher stiffness, which is why it effectively reduces strain growth rate. However, this trend was maintained for the mixture with AC 16W grain size with a fibre length of up to 3 cm and a share of up to 0.6%. Higher lengths and shares of geogrid fibres resulted in a significant increase in WTS_{air}, decreasing the rutting resistance of asphalt concrete. In the case of the glass geogrid added to asphalt concrete, the average median was higher than the general median and the median for the reference specimens. Thus, the glass geogrid increases the susceptibility to creep in asphalt concrete. Only for the AC 22 mixture with a glass fibre content of up to 0.2% and a fibre length of up to 1 cm was the result similar to the median of WTS_{air} results for specimens with the carbon geogrid.

Another considered property was water resistance *ITSR*. In addition to the physical and mechanical properties, an important issue was to describe asphalt concrete regarding its resistance to climatic factors. The aggregated results of *ITSR* tests are shown in Fig. 7.

It should be noted (Fig. 7) that the carbon geogrid was much more advantageous for the *ITSR* parameters than the glass fibres. In comparison to the reference specimens, the increase in *ITSR* in asphalt concrete with glass fibres or carbon fibres was approximately 15%. Also, the range of variability in mixtures with carbon geogrid was much smaller than for the mixtures with glass geogrid fibres. Due to the scatter of the results in the mixtures with glass fibres, the stability of *ITSR* is strongly dependent on the roughness and condition of the glass geogrid surface. In comparison with the carbon geogrid, asphalt concrete containing fibres from recycled glass geogrid has a smaller value of the parameter in most cases than the value determined for the reference specimens.

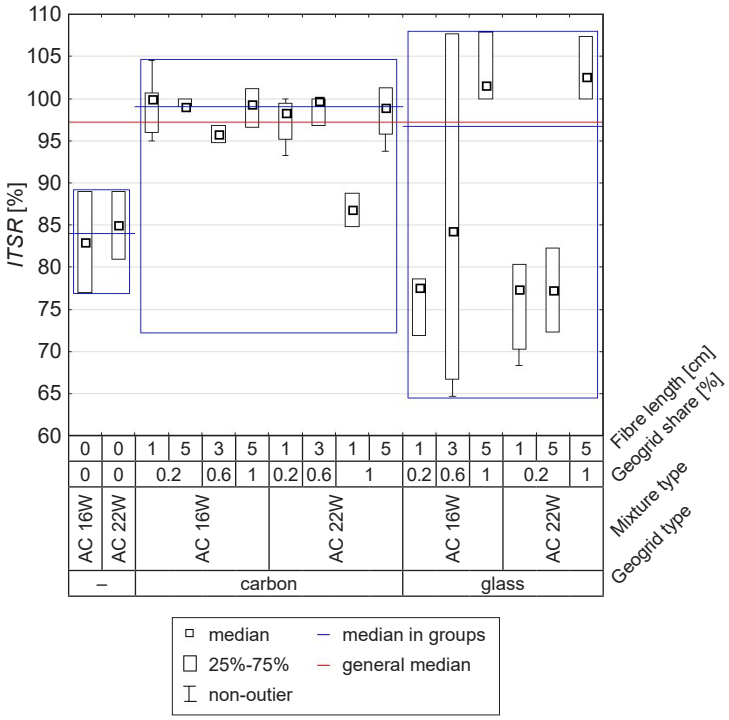

Fig. 7. Resistance of asphalt concrete to water and frost (climatic factors)

4.3. IMPACT OF RECYCLED GEOGRID ON FRACTURE TOUGHNESS

The fracture toughness of asphalt mixtures is an area of research that is currently under intensive development. The susceptibility of asphalt mixtures to cracking often determines their suitability and directly impacts the service life of the constructed pavement [28]. Scientific papers in Poland do not include any criteria for the SCB method that would enable the discrimination of mixtures with inadequate fracture toughness. According to the FHWA/LA/536 report, it was established that *J*-integral > 0.5 kJ/m^2 guaranteed satisfactory fracture toughness. Based on the preliminary analysis, the authors identified a redundant variable referred to as *P*-indicator relative to the *J*-integral. This means that the *P*-indicator can be represented using K_{Ic} after linear transformation. Consequently, the analysis of the results of fracture toughness was shown graphically for K_{Ic} and the *J*-integral on Fig. 8.

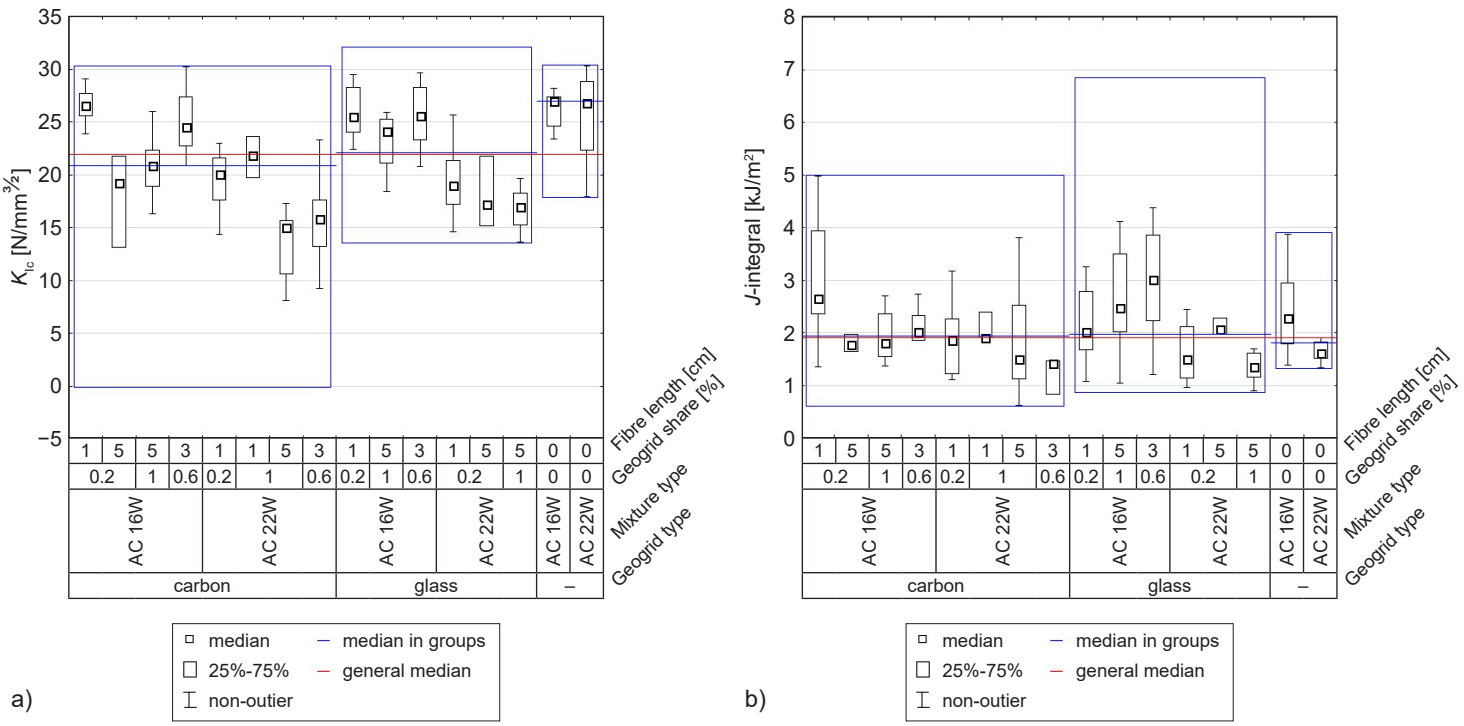

Fig. 8. SCB fracture toughness of asphalt concrete: a) K_{Ic}, b) *J*-integral

The dispersion of results on Fig. 8 indicates that the K_{Ic} parameter was significantly better for the discrimination of asphalt concrete than the *J*-integral. According to the criterion of FHWA/LA/536 regarding the value of the *J*-integral, the risk of cracking only existed for the AC 22W mixture with fibres with a length of 5 cm. In the remaining cases, the *J*-integral was higher than 0.5 kJ/m^2. The results of the K_{Ic} parameter in Fig. 8a show that its value was the most advantageous for AC 16W mixtures. For the AC 22W mixtures, apart from the reference mixtures, the results of K_{Ic} were lower than the general median. AC 16W mixtures with the highest K_{Ic} were the ones with glass geogrid. The result for this fibre type was comparable with the reference mixture, with a maximum fibre length of 5 cm and 1% share. For the carbon geogrid, in turn, the acceptable share of recycled geogrid fibres was 0.2%, with a fibre length of up to 1 cm. The remaining combinations of recycled geogrid share, particularly for AC 22W, resulted in a decrease in fracture toughness in comparison with the reference mixture.

The distribution of *J* (Fig. 8b) confirms the observations made based on the analysis of K_{Ic}. The comparison of the asphalt concrete mixture to the general median, which overlaps with the median of reference mixture specimens, indicates that only the use of the recycled glass geogrid guaranteed an increase in *J*. Thus, the released elastic energy for these mixtures would be lower than in the reference mixtures, increasing their cracking rate. In the case of the recycled carbon geogrid, only a small share, smaller than 0.2%, could improve the fracture toughness of asphalt concrete. It should be added that the acceptable recycled geogrid share < 0.2% is reasonable only if the fibre length is smaller than 1 cm. The remaining combinations not only did not increase the *J*-integral but, most importantly, reduced this parameter.

It should be noted that the analysis mainly consisted of the comparisons of the central measures (medians). Every combination of the share of recycled geogrid had its own scatter of results. Consequently, it is impossible to directly assess the quality of asphalt concrete by only referring to fracture toughness without eliminating the cases where the mixture has an insufficient resistance to permanent deformation or where it does not meet the requirements of the standards. Consequently, multi-dimensional techniques were used for further analysis.

4.4. MULTI-DIMENSIONAL ANALYSIS OF THE FRACTURE TOUGHNESS OF ASPHALT CONCRETE

The impact of fibres from the recycled geogrid on the properties of asphalt concrete in the context of fracture toughness was analysed using a multi-dimensional principal component analysis (PCA) [34, 35]. Based on the analysis, the data were clustered using the *k*-means method described in detail in the papers [36, 37]. The primary objective of the first stage of the principal component analysis was to identify the relationship between the variables. The *k*-means technique, in turn, which was the second stage of the data analysis, was used to identify homogeneous clusters characterising the quality of asphalt concrete mixtures. Regarding the first stage of the tests, using the Kaiser criterion [38], it was found that a significant representation of the data set could be obtained by defining four principal components. Each of them identified characteristic relationships with a representativity of 80.1%. The projection of the investigated properties in a new factorial space including the two most important factorial variables was shown in Fig. 9.

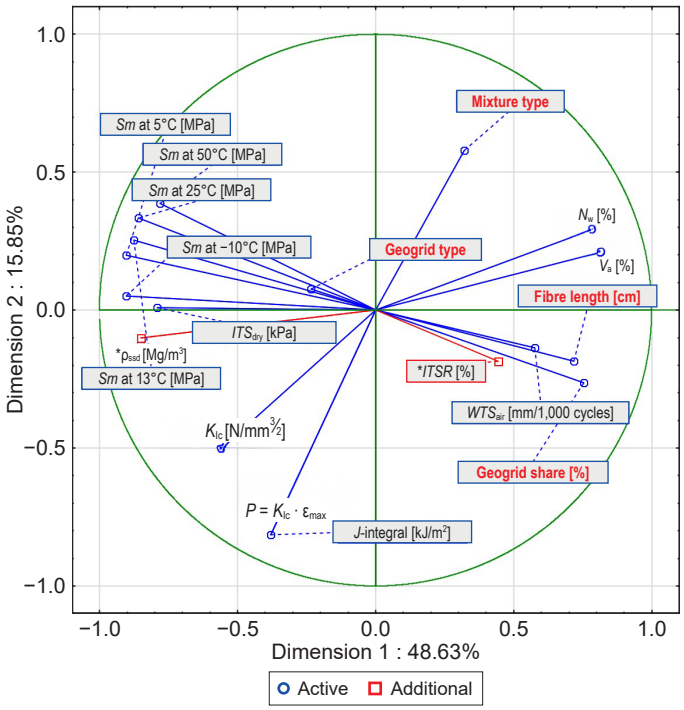

Fig. 9. Factorial space of the PCA of factor 1 and factor 2

Active variables (Fig. 9) refer to the variables that were instrumental in the formulation of the new orthogonal space, characterized by factor 1 and factor 2, thereby

serving as explanatory variables. Conversely, additional variables denote those that were excluded from consideration during the computation of the new principal component space. Nevertheless, acknowledging the significance of their presence, the computed loads associated with these variables have been subsequently projected onto a new space delineated by the active variables. The relationships in Fig. 9 indicate that the first two factors (denoted as dimension of No. 1 and No. 2) explain approximately 63% of the entire variability in the set. The length and direction of the vectors determine the strength of the impact and the correlation between the variables and each other and between the factorial variables. In a factorial analysis, it is important to interpret new factorial variables. The identification of hidden relationships in the set using the PCA method consists in finding new factorial variables that show maximum correlation with selected dependent (measured) variables and minimum correlation with other factorial variables [35]. Fig. 9 shows the relationship between two dependent variables and the factorial variables. The magnitude of the vectors signifies the degree of their association with the newly defined factor variables. Conversely, the proximity of vectors (points) is indicative of a stronger positive correlation among variables representing the attributes of the recycled mixture. For instance, strong positive correlations are observed in the context of assessing the modulus of rigidity across various temperatures, whereas an inverse correlation is noted between the modulus of rigidity and feature V_a. Consequently, a shorter vector length denotes a lower efficacy of a particular feature's influence within the context of the newly established orthogonal space [35]. The analysis was complemented by the expanded correlation table shown in the form of Table 4.

Based on Fig. 8 and Table 4, the authors identified 4 characteristic properties of the set. Factor 1 showed how the geogrid share and fibre length affected the mechanical properties of asphalt concrete. The range of variability expressed by factor 1 was approximately 49%. Based on information provided by factor 1, it can be found that an increase in fibre length and fibre share resulted in the greatest reduction of stiffness moduli *Sm* 13°C (−0.91) and *Sm* 5°C (−0.94) and the cohesion of asphalt concrete ITS_{dry} (−0.81). Also, the increase in geogrid length and share strongly reduces AC resistance to permanent deformation WTS_{air} and increases V_a. Thus, the first factor can be interpreted as: "physical properties of geogrid fibres vs mechanical properties of asphalt concrete". Factor 2, explaining 15.9% of the variability of the entire set, characterised the relationship between the geogrid type and fracture toughness expressed by the K_{Ic} parameter of asphalt concrete. The correlations assigned to factor 2 indicate that the glass geogrid had a more advantageous impact on stiffness at > 25°C ($r > 0.4$) but reduced the fracture toughness of AC, particularly the K_{Ic} parameter (−0.77), in comparison with the carbon geogrid. Consequently, it should have the following name: "geogrid type vs AC fracture toughness". It should be noted that the correlation of the variables associated with factor 2 is a much more effective identifier of the strength of the relationship between *Sm* and K_{Ic} than the impact of geogrid type ($r = -0.43$) on fracture toughness. Factor 3, explaining 9.1% of the variability, determines how the geogrid type, fibre length and fibre share affect the *J*-integral. Factor 3 complemented the information isolated by factor 2. Based on the correlations, factor 3 can be interpreted as: "rate of energy release and geogrid properties". Consequently, factor 3 indicates that the higher the share in glass geogrid fibres and the longer the fibres, the higher the possible value of the *J*-integral. This observation is consistent with the conclusions arising from the interpretation of Fig. 7b, and it justifies the division of set variability into factors. Factor 4, explaining 6.6% of the variability, identified the relationship between the grain size distribution of the AC mixture and its water resistance *ITSR*. According to the identified trend, the finer the AC mixture, the higher the *ITSR*.

All the presented analyses of test results indicate that the application of a specific share of recycled geogrid could have a positive effect by increasing the fracture toughness and imbuing the mixture with functional properties and durability in the form of a high *Sm* modulus and low WTS_{air}. However, the PCA has only provided evidence of the presence of certain advantageous relationships between the variables, but it does not provide quantitative measures in the context of the share of recycled geogrid. Proceeding to stage 2 of the data analysis, the authors used the information from the PCA to cluster the test results using the *k*-means method. It was eventually determined, using the cross-validation technique, that the division of the sample into 3 significant groups was sufficient. The graphical result of the clustering using cross-validation is shown in Fig. 10.

Table 4. Factorial coordinates of the variables (correlations)

Variable	Factor 1	Factor 2	Factor 3	Factor 4
Geogrid type (0 – glass, 1 – carbon)	−0.213149	**−0.425156**	**−0.781848**	0.010972
Mixture type (0 – AC 16W, 1 – AC 22W)	0.045366	−0.068086	0.220269	**−0.918975**
Geogrid share [%]	**0.789129**	0.011775	**0.462314**	0.195138
Fibre length [cm]	**0.736802**	0.109691	**0.438128**	−0.065708
V_a [%]	**0.874253**	0.034495	−0.200021	−0.267735
N_w [%]	**0.710514**	0.294262	−0.161139	−0.139601
ITS_{dry} [kPa]	**−0.815918**	0.033019	0.248451	−0.112936
ITSR [%]	0.507082	0.164184	0.201029	**0.412300**
Sm at −10°C [MPa]	**−0.899713**	−0.105528	0.124896	−0.000603
Sm at 5°C [MPa]	**−0.942070**	0.016322	0.022037	−0.045945
Sm at 13°C [MPa]	**−0.916481**	0.234353	0.023355	0.013751
Sm at 25°C [MPa]	**−0.879165**	**0.404873**	−0.020181	0.044008
Sm at 50°C [MPa]	**−0.762113**	**0.525579**	−0.121622	0.120673
K_{Ic} [N/mm$^{3/2}$]	−0.447065	**−0.774194**	0.113613	−0.019266
J-integral [kJ/m^2]	−0.472512	**−0.517893**	**0.433630**	0.205853
WTS_{air} [mm/1,000 cycles]	**0.682114**	−0.252606	−0.139919	0.232484
% of all explained variance	48.63	15.85	9.12	6.55

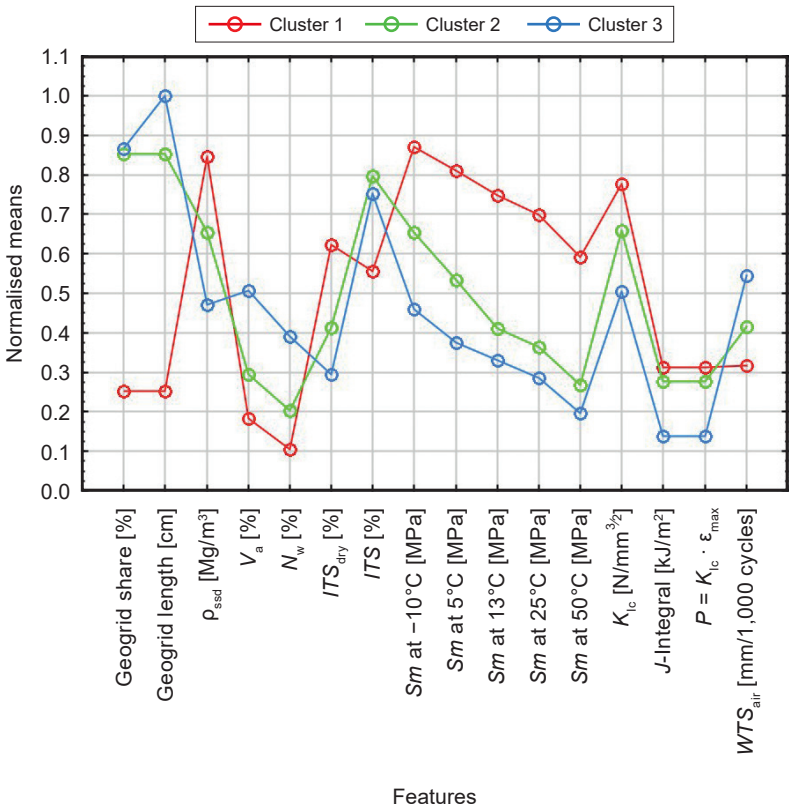

Fig. 10. Results of clustering using the *k*-means method

The results of clustering in Fig. 10 indicate that the most advantageous convergence from the perspective of functional properties existed for the asphalt concrete mixtures of group 1. These were the mixtures with the lowest V_a, a high stiffness *Sm*, the highest fracture toughness K_{Ic} and the highest rutting resistance from among all mixtures. Mixtures of group 1 had the lowest *ITSR*. Group 2 includes mixtures with intermediate properties relative to the asphalt concrete of groups 1 and 3. Asphalt concrete mixtures of the second group could be used as an alternative to group 1. The specimens of asphalt concrete of group 3 were the mixtures with properties opposite to those recorded for the mixtures of group 1. Their only advantage was the highest resistance to water and frost *ITSR*. The potential use of asphalt concrete with the properties represented by group 3 depends on the fulfilment of the requirements defined by WT-2/2014 [3]. The characteristics summarising the average value of a specific property qualified into a specific group, with a 95% confidence interval, are given in Table 5.

Property	Group 1	Difference between group 1 and AC ref.	Group 2	Difference between group 2 and AC ref.	Group 3	Difference between group 3 and AC ref.
V_a [%]	4.01 ± (0.74)	−16.6	5.35 ± (2.08)**)	11.4	7.91 ± (4.39)*)	64.5
ITS_{dry} [kPa]	1,937.13 ± (275.82)	20.0	1,465.01 ± (235.85)	−9.2	1,199.81 ± (643.95)	−25.7
ITSR [%]	88.63 ± (8.53)	5.5	99.08 ± (5.31)	18.0	97.13 ± (13.99)	15.6
Sm at −10°C [MPa]	30,298.47 ± (1619.27)	1.6	22,898.77 ± (5083.08)	−23.2	16,293.58 ± (13166.61)	−45.3
Sm at 5°C [MPa]	20,038.21 ± (1740.95)	−8.3	14,614.68 ± (4117.1)	−33.1	11,526.94 ± (7606.92)	−47.2
Sm at 13°C [MPa]	14,655.11 ± (1302.24)	4.5	9,620.29 ± (3321.83)**)	−31.4	8,425.83 ± (5150.69)**)	−39.9
Sm at 25°C [MPa]	7,128.45 ± (828.4)	13.2	4,492.67 ± (1629.59)	−28.6	3,879.31 ± (2112.06)	−38.4
Sm at 50°C [MPa]	1,136 ± (217.52)	19.3	640.84 ± (347.26)	−32.7	530.25 ± (356.39)	−44.3
K_{Ic} [N/mm$^{3/2}$]	23.46 ± (3.79)	−8.2	19.85 ± (3.53)	−22.3	15.26 ± (4.86)	−40.3
J−integral [kJ/m^2]	2.42 ± (0.68)	7.1	2.22 ± (1.14)	−2.0	1.42 ± (0.79)	−37.3
$P = K_{Ic} \cdot \varepsilon_{max}$	37.51 ± (10.59)	7.1	34.31 ± (17.61)	−2.0	21.95 ± (12.25)	−37.3
WTS_{air} [mm/1,000 cycles]	0.06 ± (0.01)	−9.8	0.07 ± (0.02)	5.9	0.09 ± (0.04)	26.8
Geogrid share [%]	0.25 ± (0.13)	–	0.85 ± (0.26)	–	0.87 ± (0.4)	–
Fibre length [cm]	1.26 ± (0.64)	–	4.26 ± (1.32)	–	5 ± (0)	–

*) does not meet the requirements of WT-2/2014 [3],
**) below the reference level of the property specified in the KTKNPiP [32]

In analysing the results in Table 5, it should be noted that the results of group 3 did not meet the requirements of WT-2/2014 [3] for parameter V_a and had *Sm* at 13°C lower by 40% on average than the reference value not modified with geogrid fibres. Also, in group 3, the average WTS_{air} in specimens containing geogrid fibres was 27% higher, and the value of the *J*-integral – 38% lower than in the reference mixtures. In group 2, the average value of V_a achieved the required level in the range of 4% to 6%. Regarding the confidence interval of the property V_a, in turn, there is a high risk that asphalt concrete specimens will achieve values outside the required range. Similarly to group 3, in group 2, the average stiffness at 13°C is lower than the reference stiffness in KTKNPiP [32], i.e., *Sm* = 10,300 MPa. In group 2, ITS_{dry} has increased significantly by 18% relative to the reference asphalt concrete. In summary, group 1 had the most advantageous values from the perspective of the requirements of WT-2/2014. Group 1 included AC specimens with the lowest *ITSR*, which, however, still conformed to the requirements of WT-2/2014 [3]. Also, the increase in ITS_{dry} was 20% higher and in WTS_{air} – 10% lower than the results for the reference specimens. Also, the rate of energy release *J* was 7% lower in the specimens of group 1 in relation to the reference mixtures. To conclusively determine the safe share of recycled geogrid fibres, the identified clusters of test results were projected depending on stiffness *Sm* at 13°C and K_{Ic}. The graphical interpretation of the projection is shown in Fig. 11.

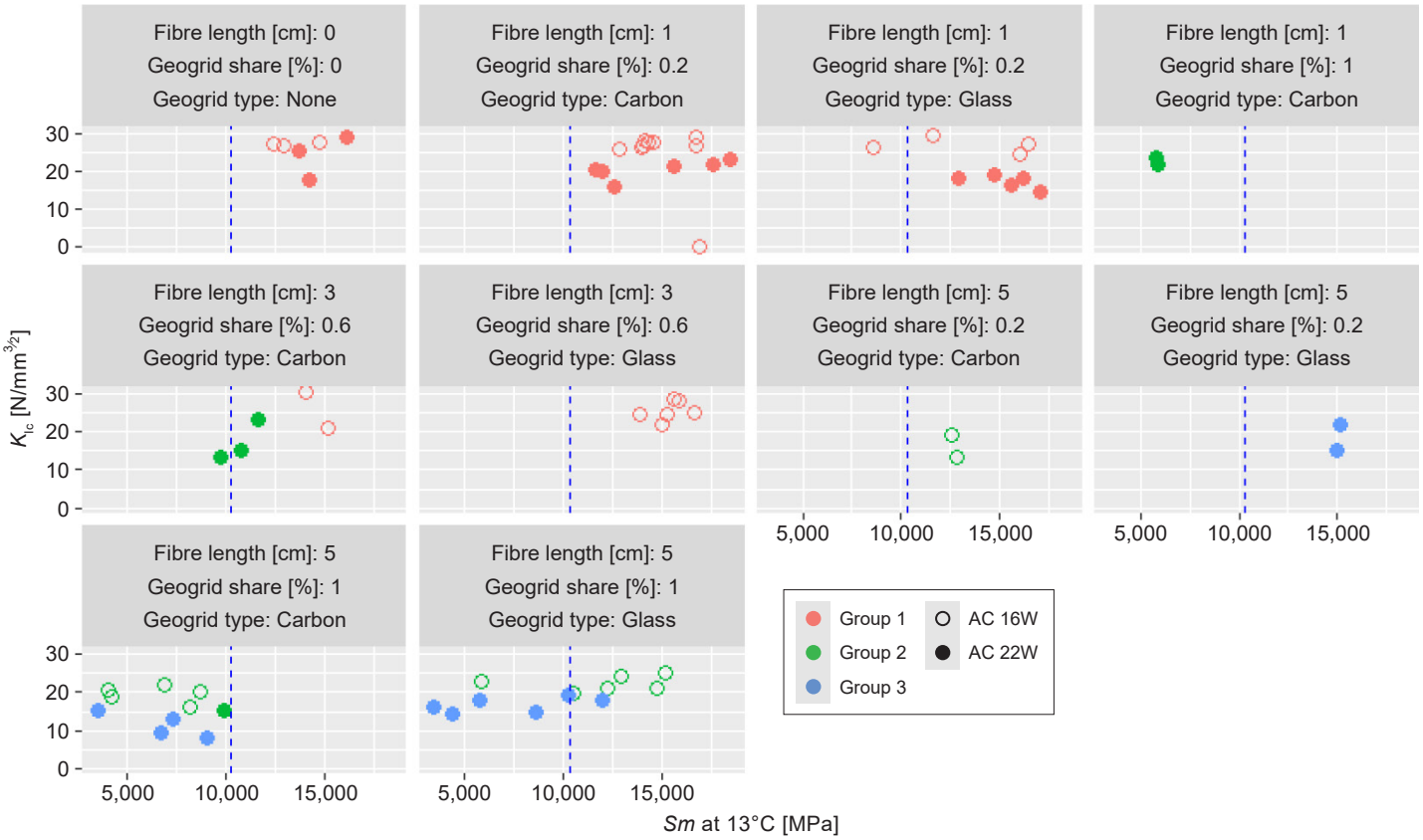

Fig. 11. Results of clustering depending on K_{Ic} and *Sm* at 13°C

The results of clustering shown in Fig. 11 provided valuable information about the relationship between AC fracture toughness and the design parameter: *Sm* stiffness at 13°C (the dashed blue line represents 10,300 MPa). The clustering charts shown in Fig. 10 indicate that the recommended share of glass and carbon geogrid fibres was < 0.2%, with a fibre length < 1 cm, regardless of the grain size distribution of the mixture. Group 1 also included the reference mixtures of asphalt concrete. It should be noted, however, that the AC 16W mixtures had higher fracture toughness K_{Ic} than AC 22W. An acceptable quality of asphalt concrete can be achieved also using fibres with a length of up to 3 cm and a share of up to 0.6%. However, this is possible for the AC 16W mixture only if it is made using glass fibres. Increasing fibre length > 1 cm and fibre share > 0.2% for the carbon geogrid decreases AC quality, causing the mixture to be classified as group 2. Using fibres with a share > 1% and a length of 1-5 cm causes the quality of the mixtures to decrease to an unacceptable level represented by group 3, particularly for AC 22 mixtures. In the case of the AC 16 mixture, it is possible to use fibres with a length > 3 cm and a share > 0.6%, but this presents a risk of exceeding the $V_{a\ limit}$, making the mixture difficult to compact.

5. CONCLUSIONS

The tests and analyses support the following conclusions:

1. The surveys showed that plastic geogrid was the second-largest impurity observed by the respondents during the milling of asphalt mixtures.
2. A controlled share of recycled geogrid increases the stiffness of asphalt concrete, particularly at high service temperatures.
3. Glass geogrid improves the indirect tensile strength and water resistance. The most important advantage of the carbon fibre geogrid, in turn, was the reduced rut deformation rate.
4. The key factor improving the fracture toughness of asphalt concrete was the type of material used to make the geogrid. The use of glass fibre geogrid was more advantageous for the properties of asphalt concrete than the carbon geogrid.

5. The tests showed that geogrid fibres, regardless of the material they were made of, in the share of up to 0.3% with a fibre length of up to 1 cm, significantly increased the capability of asphalt concrete to absorb energy before crack propagation J-integral in comparison with the reference mixture.
6. Based on the analysis of the clustering, it was found that the use of geogrid with a share of up to 0.6% and a fibre length of 3 cm in the AC 16W mixture reduced the strain rate WTS_{air} by approximately 10%, increased the *J*-integral by 7%, increased *Sm* at temperatures over 13°C by 13% and increased ITS_{dry} by 20% in comparison with the reference mixture. The same effect could be achieved for carbon fibres, but with a fibre content of up to 0.2% and fibre length of up to 1 cm.

In summary, drawing upon a statistical multivariate analysis, the most secure percentage range of fibers in the domain is ≤ 0.6% m/m with a length of ≤ 3 cm (independent of AC 16W/AC 22W). Nevertheless, this might necessitate supplementary conditions:

- The fractionation of Reclaimed Asphalt Pavement (RAP) should be conducted at the facility. This process entails an initial separation of fractions containing large fragments, with optional further comminution and regulation of fiber content within the RAP stream, in alignment with standardized protocols QIP-129.
- Enhanced Quality Control/Quality Assurance (QC/QA) measures ought to be implemented, alongside the establishment of a Reclaimed Asphalt Pavement (RAP) acceptance specification, comprising: 1) a constraint on fiber content not exceeding 0.6% *w*/*m* within the recycled mixture and 2) a requirement for the probability of observing a fiber length of $P(L < 10$ cm) to equal or exceed 90%.
- Optionally, the fracture toughness may be confirmed by establishing a threshold of $Jc \geq 0.5$ kJ/m^2 for the control specimens.

REFERENCES

[1] Gospodarka o obiegu zamkniętym: definicja, znaczenie i korzyści. Tematy, Parlament Europejski, 2023 https://www.europarl.europa.eu/topics/pl/article/20151201STO05603/gospodarka-o-obiegu-zamknietym-definicja-znaczenie-i-korzysci-wideo (available: 01.10.2025)

[2] Asphalt in Figures 2022. European Asphalt Pavement Association, Brussels, Belgium, 2024, https://asefma.es/wp-content/uploads/2024/02/asphalt-in-figures-2022-regular.pdf (available: 01.10.2025)

[3] WT-2 Nawierzchnie asfaltowe na drogach krajowych. Część I: Mieszanki mineralno-asfaltowe, Wymagania techniczne. GDDKiA, Warszawa, 2014 (in Polish)

[4] PN-EN 13108-8:2008 Bituminous mixtures – Material specifications – Part 8: Reclaimed asphalt

[5] *Kowalczyk A.*: Wpływ geosiatki pochodzącej z recyklingu nawierzchni asfaltowej na trwałość betonu asfaltowego. Ankieta badawcza pracy doktorskiej, Politechnika Świętokrzyska, Kielce, 2023 (in Polish)

[6] *Bugajski M.*, Grabowski W.: Geosyntetyki w budownictwie drogowym. Wydanie I. Wydawnictwo Politechniki Poznańskiej, Poznań, 1999 (in Polish)

[7] *Wu S.*, *Haji A.*, *Adkins I.*: State of art review on the incorporation of fibres in asphalt pavements, Road Materials and Pavement Design, **24**, 6, 2022, 1559-1594, DOI: 10.1080/14680629.2022.2092022

[8] *Gogolin D.*: Wirkung und Nachhaltigkeit von Asphaltarmierungen. S&P Clever Reinforcement GmbH, Expert Report: 14-7974-01, Frankfurt, Germany, 2015 (in German)

[9] Gesetz zur Förderung der Kreislaufwirtschaft und Sicherung der umweltverträglichen Bewirtschaftung von Abfällen (Kreislaufwirtschaftsgesetz – KrWG). Bundesministerium der Justiz, Berlin, Germany, 2012 (in German)

[10] *Shanbara H.K.*, *Ruddock F.*, *Atherton W.*: A laboratory study of high-performance cold mix asphalt mixtures reinforced with natural and synthetic fibres, Construction and Building Materials, **172**, 2018, 166-175, DOI: 10.1016/j.conbuildmat.2018.03.252

[11] *Lin Y.*, *Karadelis J.N.*: Establishing the fiber bridging law by an inverse analysis approach. Journal of Materials in Civil Engineering, **28**, 2, 2016, Article ID: 04015105, DOI: 10.1061/(ASCE)MT.1943-5533.0001386

[12] *Miao Y.*, *Wang T.*, *Wang L.*: Influences of interface properties on the performance of fiber-reinforced asphalt binder. Polymers, **11**, 3, 2019, Article ID: 542, DOI: 10.3390/polym11030542

[13] *Apostolidis P.*, *Liu X.*, *Daniel G.C.*, *Erkens S.*, *Scarpas T.*: Effect of synthetic fibres on fracture performance of asphalt mortar. Road Materials and Pavement Design, **21**, 7, 2020, 1918-1931, DOI: 10.1080/14680629.2019.1574235

[14] *Mazurek G.*, *Buczyński P.*, *Kowalczyk A.*: The effect of recycled geogrid fibres on asphalt concrete performance: A case study from Poland. Materials, **17**, 23, 2024, Article ID: 5923, DOI: 10.3390/ma17235923

[15] PN-EN 15381:2010 Geotextiles and geotextile-related products – Characteristics required for use in pavements and asphalt overlays

[16] *Montgomery D.C.*: Design and analysis of experiments. Eighth edition. John Wiley & Sons, Hoboken, NJ, 2013

[17] *Lazić Ž.R.*: Design of experiments in chemical engineering: A practical guide. Wiley-VCH: Weinheim, Germany, 2004

[18] *Nelder J.A.*, *Wedderburn R.W.M.*: Generalized linear models. Journal of the Royal Statistical Society. Series A (General), **135**, 3, 1972, 370-384, DOI: 10.2307/2344614

[19] PN-EN 12697-8:2005 Bituminous mixtures – Test methods – Part 8: Determination of void characteristics of bituminous specimens

[20] PN-EN 12697-12:2008 Bituminous mixtures – Test methods – Part 12: Determination of the water sensitivity of bituminous specimens

[21] PN-EN 1097-6:2013 Tests for mechanical and physical properties of aggregates – Part 6: Determination of particle density and water absorption

[22] PN-EN 12697-23:2009 Bituminous mixtures – Test methods – Part 23: Determination of the indirect tensile strength of bituminous specimens

[23] PN-EN 12697-26:2012 Bituminous mixtures – Test methods for hot mix asphalt – Part 26: Stiffness

[24] PN-EN 12697-22:2008 Bituminous mixtures – Test methods – Part 22: Wheel tracking

[25] PN-EN 12697-44:2010 Bituminous mixtures – Test methods for hot mix asphalt – Part 44: Crack propagation by semi-circular bending test

[26] PN-EN 12697-33:2008 Bituminous mixtures – Test methods for hot mix asphalt – Part 33: Specimen prepared by roller compactor

[27] *Rice J.R.*: A path independent integral and the approximate analysis of strain concentration by notches and cracks. Journal of Applied Mechanics, **35**, 1968, 379-386, http://esag.harvard.edu/rice/015_Rice_PathIndepInt_JAM68.pdf (available: 01.10.2025)

[28] *Szydłowski C.*, *Judycki J.*: Badania odporności na pękanie mieszanek mineralno-asfaltowych na próbkach półwalcowych. Drogownictwo, **70**, 10, 2015, 348-353 (in Polish)

[29] *Szydłowski C.*, *Dołżycki B.*: Investigation of mineral-cement-emulsion (MCE) road subbase fracture parameters. Materiały Budowlane, 10, 2017, 83-87, DOI: 10.15199/33.2017.10.28 (in Polish)

[30] *Błażejowski K.*, *Tabor Z.*, *Wójcik-Wiśniewska M.*, *Zduńczyk B.*, *Baranowska W.*: Warstwy przeciwspękaniowe z asfaltem wysoko modyfikowanym ORBITON HIMA. Konferencja „Nowoczesna diagnostyka i naprawy nawierzchni drogowych", Kielce 2018 (in Polish)

[31] *Artamendi I.*, *Khalid H.A.*: A comparison between beam and semi-circular bending fracture tests for asphalt. Road Materials and Pavement Design, **7**, sup1, 2006, 163-180, DOI: 10.1080/14680629.2006.9690063

[32] *Judycki J.*, *Jaskuła P.*, *Pszczoła M.*, *Alenowicz J.*, *Dołżycki B.*, *Jaczewski M.*, *Ryś D.*, *Stienss M.*: Katalog Typowych Konstrukcji Nawierzchni Podatnych i Półsztywnych. GDDKiA, Warszawa, 2014 (in Polish)

[33] *Han J.*, *Zhao M.*, *Chen J.*, *Lan X.*: Effects of steel fiber length and coarse aggregate maximum size on mechanical properties of steel fiber reinforced concrete. Construction and Building Materials, **209**, 2019, 577-591, DOI: 10.1016/j.conbuildmat.2019.03.086

[34] *Dąbrowski J.*: O problemie redukcji wymiarów (dla niestatystyków). Polskie Towarzystwo Inżynierii Rolniczej, Kraków 2000 (in Polish)

[35] *Stanisz A.*, *Tadeusiewicz R.*: Przystępny kurs statystyki z zastosowaniem STATISTICA PL na przykładach z medycyny. **T.2**, StatSoft Polska, Kraków 2007 (in Polish)

[36] *Hartigan J.A.*: Clustering algorithms. John Wiley & Sons, New York, 1975

[37] *Mazurek G.*, *Iwański M.*: Multidimensional analysis of the effects of waste materials on physical and mechanical properties of recycled mixtures with foamed bitumen. Applied Sciences, **8**, 2, 2018, Article ID: 282, DOI: 10.3390/app8020282

[38] *Kaiser H.F.*: The varimax criterion for analytic rotation in factor analysis. Psychometrika, **23**, 1958, 187-200

Wpływ geosiatki szklanej i węglowej z recyklingu na odporność na propagację spękań betonu asfaltowego

Streszczenie: W artykule przedstawiono analizę wpływu włókien z geosiatki pochodzącej z recyklingu na właściwości mechaniczne i fizyczne betonu asfaltowego. Wykonane badania ankietowe wskazują, że stan wiedzy w tym zakresie jest bardzo ograniczony. Natomiast obecność włókien geosiatki uzyskiwanej w procesie frezowania jest coraz częstszym problemem, z którym należy się zmierzyć w trakcie projektowania nowych nawierzchni z mieszanek mineralno-asfaltowych (mma) zawierających w swoim składzie granulat asfaltowy. Przyjęty proces badawczy obejmował selekcję i optymalizację zawartości dodatku geosiatki z recyklingu pochodzenia szklanego i węglowego do mma. Zaprojektowano dwie referencyjne mieszanki z betonu asfaltowego, przeznaczonego do warstwy wiążącej AC 16W 35/50 KR3-4 i AC 22W 35/50 KR3-4. Proces badawczy był kontrolowany za pomocą czynnikowego planu eksperymentu, uwzględniającego dwie zmienne jakościowe: rodzaj geosiatki i uziarnienie mieszanki mineralnej oraz dwie zmienne ilościowe: udział procentowy oraz długość włókna geosiatki. Zaprojektowane i przygotowane w warunkach laboratoryjnych mieszanki poddano zasadniczemu badaniu odporności na propagację spękań przy wykorzystaniu metody SCB. Ponadto badania obejmowały również ocenę cech towarzyszących: wolnej przestrzeni V_a, wrażliwości na działanie wody *ITSR*, odporności na koleinowanie PRD_{air}, WTS_{air}. Wyniki analiz pozwoliły stwierdzić, że potencjalnie istnieje możliwość poprawy odporności na pękanie betonu asfaltowego, przeznaczonego do warstwy wiążącej poprzez optymalizację parametrów geosiatki. Ponadto, możliwość wykorzystania recyklowanej geosiatki do produkcji mma stwarza warunki do stosowania założeń zasady zrównoważonego rozwoju w branży budowlanej o specjalności drogowej.

Słowa kluczowe: geosiatka z recyklingu, odporność na spękanie, optymalizacja, plan eksperymentu, recykling.